EAI Endorsed Transactions
on Industrial Networks and Intelligent Systems
Research Article EAI.EU

Information Outage Probability and Constrained Capacity of Moderate-Length Codes over AWGN Channels*

Lan K. Nguyen[1], Duy H. N. Nguyen[2], Richard Wells[3], and Nghi H. Tran[4,*]

[1]Linquest Corporation, CA, USA
[2]Department of Electrical and Computer Engineering, San Diego State University, CA, USA
[3]University of Idaho, Idaho, USA
[4]Department of Electrical and Computer Engineering, University of Akron, OH , USA

Abstract

We study the information outage probability (IOP) and constrained capacity of moderate-length codes over AWGN channels based on M-ary phase-shift keying signals. The IOP provides an important benchmark for performance evaluation of moderate-length codes. We analytically compute the IOP and compare it with numerical simulations using the DVB-S2 error-correcting code with numerous code rates employed in Protected Tactical Waveform (PTW). Numerical results confirm the tightness of the analytical results.

Received on 03 October 2021; accepted on 01 November 2021; published on 03 November 2021

Keywords: Moderate-length codes, Mutual information, Outage capacity, DVB-S2, SATCOM.

doi:10.4108/eai.3-11-2021.171755

1. Introduction

From the information theoretic measure, channel capacity provides a fundamental understanding of the performance on a signaling type over a channel. It addresses the problem of efficient data transmission over the channel. Channel capacity is closely related to mutual information, which provides a reduction in uncertainty about the channel input given the knowledge of the channel output. Wide classes of channels have been studied based on probability theory such as ergodic theory or laws of large numbers. In order to establish the channel capacity or ergodic channel capacity result, the code block length is allowed to grow without bound. Channel capacity is related to the average mutual information only in the limit of infinite-length codewords. If the coding length is required to be infinite for the average mutual information to converge, then one might infer that the real value of interest is not the average mutual information, but the mutual information itself. Also, recent results on channel capacity for a general class of channels; the average mutual information is not sufficient for that purpose [2]. This observation motivates us to study mutual information itself, which then provides insight into the performance of finite-length codewords.

In the early development of information theory, mutual information between the channel input and output is treated as a random variable [2–4]. The failure probability or the information outage probability (IOP), is defined as the probability of this random variable drops below the code rate R [5]. The IOP is simply referred as the outage probability in this paper. A formal approach of IOP was presented in Feinstein's Lemma [4], which states that a code exists with maximal codeword error probability that is incrementally higher than the IOP. Feinstein's Lemma suggests that the IOP could be used as a benchmark for the codeword error probability. In previous works, authors focused IOP on fading channel [6, 7]. In this model, each codeword is divided into K timeslots, each of duration T, and each timeslot is transmitted through a fading channel. The signal to noise ratio (SNR) is assumed to be constant

★A part of this work was presented at IEEE Military Communications Conference, Los Angeles, CA, USA, October 2018 [1].
*Corresponding author. Email: nghi.tran@uakron.edu

in each timeslot but may vary from one timeslot to the next timeslot. The overall mutual information is found by averaging across K timeslots [8–10]. In general, IOP does not provide a lower decoding bound [8, 11]. It bounds on the maximum probability of error, not the average probability of error. It provides a good performance benchmark of the achievable decoding error rates. For this reason, the performance bound simply means the performance benchmark in this paper.

In the regime of finite-length codes, the IOP also appeared in the literature in the context of information spectrum methods [2, 8, 12–15]. The IOP is simply the cumulative distribution function (cdf) of the mutual information rate random variable, evaluated at code rate R. The main utility of the cdf is that it can be analytically obtained by the Gaussian Q-function, instead of simulating the actual code. It, however, provides a performance guidance for the code designers.

In the regime of moderate-length codes where the number of symbols per codeword is $n > 1000$, the IOP for QPSK, LTE turbo code is discussed in [11]. A numerical method for BPSK, LTE turbo code is discussed in [16]. As shown in [11, 16], in order to achieve maximum AWGN capacity, the input signal is assumed to follow a Gaussian distribution function. Results shown in [11, 16] indicate that the IOP is about 0.7 dB and 1.2 dB better than the block error rate (BLER), respectively. Motivated by these results, we study the performance of Protected Tactical Waveform (PTW) [17, 18], which employs M-PSK signals, using Second Generation Digital Video Broadcasting Satellite (DVB-S2) forward error correcting (FEC) code with numerous code rates, and a fixed length of $16,200$ coded bits. DVB-S2 FEC is based on the concatenation of BCH (Bose-Chaudhuri-Hocquengham) and LDPC (Low Density Parity Check) codes. PTW has been adopted by the Air Force to use over the commercial and Military Satellite Communication (MILSATCOM) systems. PTW supports very high data rates while providing secured and anti-jam protection, as well as low probability of intercept and detection (LPI/LPD) [19] capability.

The IOP results obtained by previous studies [11, 16] are satisfactory only for the codes which operate in the region of low to moderate SNR where the maximum capacity or Shannon capacity matches the constrained capacity. These results rely on Gaussian distribution assumption of the input signal. However, the Gaussian input assumption results in loose performance bound for high modulation orders where FEC operates in high region of SNR [20]. The main contribution of the paper is to provide a general solution for the IOP for a wide range of SNR, which includes high orders of modulation and high code rates. We do not rely on the Gaussian distribution of the input signal. A uniform distribution is realistic and used in the paper. To best of our knowledge, this paper is the first work that examines the IOP by relaxing the Gaussian input assumption. We show that the IOP provides a very tight performance bound, specifically, the theoretical performance benchmark for PTW, a future Military Standard waveform for MILSATCOM. In the preliminary work reported in [1], we presented our approximation approach to find the IOP and constrained capacity of moderate-length codes. In this work, we provide more thorough investigation and comparison between the proposal approach to results achieved by Gaussian signaling. In the simulation section we show the Gaussian assumption results in very loose performance bound for codes that operate in the region of high SNR; it exceeds 3.6 dB for 8-PSK with code rate 8/9, while our approach results in a very tight bound, less than 0.3 dB. The results of this paper can be extended to study the performance for a wide class of codes.

The outline of the paper is as follows: In Section II, a review of mutual information, average mutual information, and mutual information rate. The calculation of IOP is based on additive Gaussian noise (AWGN) channels. There are two parts: Part I when input M-PSK signal is assumed to follow a Gaussian distribution; Part II, we relax the Gaussian distribution of the input signal and a more realistic uniform distribution is used. In part II, we show that the received signal is a Gaussian mixture. Therefore, maximum capacity is not achieved in the region of high SNR. In addition, for high orders of modulation, e.g., QPSK or higher, there is no closed form solution for the average mutual information and the information rate random variable. The calculation of IOP is based on the constrained capacity of the M-PSK signals. We present approximation and numerical integration methods to compute the constrained capacity. Details of these methods are discussed in sections II and III of the papers. Finally, simulation results using PTW which employs DVB-S2 FEC code with numerous code rates and the IOP obtained in Section II are presented in Section 2, followed by some concluding remarks in Section 3.

Notations: We use capital letters to denote random variables, small letters to indicate sample values, bold letters to indicate vectors of sample values. To simplify the analysis, complex baseband signaling is considered. In addition, codeword error rate and block error rate are used interchangeably.

2. System and Channel Model

We consider a one-to-one communication link. At the receiver, the discrete time output signal of the additive

white Gaussian channel noise is given by

$$Y = X + N \tag{1}$$

where X denotes the Gray-coded M-PSK transmitted symbols, and N denotes the additive white Gaussian noise (AWGN).

The probability density function (pdf) of the complex AWGN is given by

$$f_N(n) = \frac{1}{\pi N_0} e^{-\frac{|n|^2}{N_0}} \tag{2}$$

where N_0 denotes the noise power density. The mutual information between samples x and y is given by

$$i(x;y) = \log\left(\frac{f_{Y|X}(y|x)}{f_Y(y)}\right) \tag{3}$$

where $\log(\cdot)$ denotes the natural logarithmic function, $f_{Y|X}(y|x)$ denotes the conditional pdf of Y given X; it is given by

$$f_{Y|X}(y|x) = \frac{1}{\pi N_0} e^{-\frac{|y-x|^2}{N_0}}. \tag{4}$$

The mutual information $i(x;y)$ is a random variable with unit of nats/channel use. The average mutual information is given by

$$I(X;Y) = E\{i(x;y)\} \tag{5}$$

where $E\{\cdot\}$ denotes the expectation operator. The average mutual information (5) can also be expressed as

$$I(X;Y) = \lim_{n\to\infty} \frac{1}{n} \sum_{k=1}^{n} i(x_k;y_k). \tag{6}$$

The above expression suggests that the average mutual information can be estimated based on the mutual information of the input and output vectors of length n [8], i.e.,

$$\frac{1}{n} i(\boldsymbol{x}^n;\boldsymbol{y}^n) = \frac{1}{n} \sum_{k=1}^{n} i(x_k;y_k) \tag{7}$$

where n denotes the number of symbols per codeword. The expression on the right-hand side (RHS) of (7) is also known as the mutual information rate. Mutual information rate is a random variable.

2.1. Part I: Gaussian Distributed Input

Suppose the input random variable X is a zero-mean, complex Gaussian random variable, the pdf of X is given by

$$f_X(x) = \frac{1}{\pi E_s} e^{-\frac{|x|^2}{E_s}} \tag{8}$$

where E_s denotes the symbol energy. Since both signal X and noise N are zero-mean complex Gaussian random variables, the output signal Y is also a zero-mean complex Gaussian random variable, and the pdf of Y is given by

$$f_Y(y) = \frac{1}{\pi E_s + N_0} e^{-\frac{|x|^2}{E_s+N_0}}. \tag{9}$$

Substituting (4) and (9) into (3), the mutual information is

$$i(x;y) = \log\left(1 + \frac{E_s}{N_0}\right) + \frac{|y|^2}{E_s + N_0} - \frac{|y-x|^2}{N_0}. \tag{10}$$

Substituting (10) into (5), the average mutual information is

$$I(X;Y) = E\{i(x;y)\} = \log(1+\gamma) \tag{11}$$

where the signal to noise ratio (SNR) is given by

$$\gamma = \text{SNR} = \frac{E_s}{N_0}. \tag{12}$$

The channel capacity or the Shannon capacity for the AWGN is given by [3]

$$C^0(\gamma) = \sup_{f_X(x)} I(X;Y) = \log(1+\gamma). \tag{13}$$

As shown in (11) and (13), for AWGN channel, the maximum capacity C^0 is obtained when the pdf of X follows a Gaussian distribution.

Given that (10), (11), and (13), the mutual information rate random variable shown in (7) can be shown to have the same distribution as random variable Z_n; it is given by

$$Z_n = C^0 + W_n \tag{14}$$

where

$$W_n = \frac{1}{n} \sum_{k=1}^{n} \left(\frac{|Y_k|^2}{E_s + N_0} - \frac{|N_k|^2}{N_0}\right) \tag{15}$$

where n denotes the number of symbols per codeword. Since Y and N are zero-mean Gaussian random variables, $|Y|^2$ and $|N|^2$ are chi-square distributed random variables. For two degrees of freedom (complex data), chi-square distribution becomes exponential distribution. Furthermore, for $n = 1$, the difference of two exponentially distributed random variables is a zero-mean Laplacian random variable with variance [8, 21]

$$\sigma_w^2 = \frac{2\gamma}{\gamma+1}, \text{for } n = 1. \tag{16}$$

Again, γ is the SNR, given by (12). Using Central Limit Theorem, for large n ($n > 100$), W_n is approximated by

a Gaussian random variable. The distribution of the Z_n can be approximated as

$$Z_n \sim \mathcal{N}\left(C^0, \frac{2\gamma}{n(\gamma+1)}\right). \tag{17}$$

Proposition 1. For infinite length codeword, the mutual information rate random variable Z_n is the Shannon capacity.

Proof. Taking the limit of the variance of the mutual information rate random variable Z_n as the codeword length approaches infinity, one obtains

$$\lim_{n\to\infty} \mathrm{Var}(Z_n) = \lim_{n\to\infty} \frac{2\gamma}{n(\gamma+1)} = 0. \tag{18}$$

The mutual information rate random variable converges to the Shannon capacity. This result is consistent with (11) and (13).

The cumulative distribution function of Gaussian random variable Z_n is given by

$$F_{Z_n}(z) = Q\left(\frac{C^0 - z}{\sqrt{2\gamma/n(\gamma+1)}}\right), \tag{19}$$

where $Q(x)$ is defined as

$$Q(x) = \frac{1}{\sqrt{2\pi}} \int_a^\infty \exp\left(-\frac{t^2}{2}\right) \mathrm{d}t. \tag{20}$$

Define the code rate as

$$R_c \triangleq \frac{k}{m}, \tag{21}$$

where k denotes the number of information bits and m denotes the number of coded bits per codeword. Code rate R_c is normally specified in communications systems.

The effective code rate in bits/symbol is given by

$$R_e = R_c \log_2 M. \tag{22}$$

The outage probability P_o is the probability that the mutual information rate is less than the code rate R_e. The outage probability for Z_n is given by

$$P_o = P[Z_n \le R_e] = F_{Z_n}(R_e), \tag{23}$$

or

$$P_o = Q\left(\frac{C^0 - R_e}{\sqrt{2\gamma/\pi(\gamma+1)}}\right). \tag{24}$$

□

2.2. Part II: Uniform Input Distribution

For M-PSK communication systems, Gaussian distribution assumption for the input signal is not realistic. A more realistic distribution for X is uniform distribution; the pdf of X is given as

$$f_X(x) = \sum_{k=1}^{K} p(x_k)\delta(x - x_k) \tag{25}$$

where

$$p(x_k) = 1/M, \tag{26}$$

$\delta(\cdot)$ denotes the Dirac delta function, M denotes the size of the M-PSK alphabet, and x_k denotes the M-PSK transmitted symbol, a member of the M-PSK alphabet.

The pdf of the output random variable Y is the convolution of (2) and (25); it is given by

$$\begin{aligned} f_Y(y) &= \frac{1}{M}\int_{-\infty}^{\infty} \sum_{k=1}^{M} \delta(u - x_k) f_N(y-u)\mathrm{d}u \\ &= \frac{1}{M}\sum_{k=1}^{M} f_N(y - x_k), \end{aligned} \tag{27}$$

or

$$f_Y(y) = \frac{1}{M}\sum_{k=1}^{M} \frac{\mathrm{e}^{-\frac{|y-x_k|^2}{N_0}}}{\pi N_0}. \tag{28}$$

The mean value of the output signal is

$$\begin{aligned} E\{Y\} &= \frac{1}{MN_0\pi}\sum_{k=1}^{M}\int_{-\infty}^{\infty} y\mathrm{e}^{-\frac{|y-x_k|^2}{N_0}}\mathrm{d}y \\ &= \frac{1}{M}\sum_{k=1}^{M} x_k = 0, \end{aligned} \tag{29}$$

and the output signal power is

$$\begin{aligned} E\{Y^2\} &= \frac{1}{MN_0\pi}\sum_{k=1}^{K}\int_{-\infty}^{\infty} y^2\mathrm{e}^{-\frac{|y-x_k|^2}{N_0}}\mathrm{d}y \\ &= N_0 + \frac{1}{M}\sum_{k=1}^{M}|x_k|^2 = E_s + N_0, \end{aligned} \tag{30}$$

where

$$E_s = \frac{1}{M}\sum_{k=1}^{M}|x_k|^2. \tag{31}$$

The variance of the output signal is then given by

$$Var\{Y\} = E\{Y^2\} - [E\{Y\}]^2 = E_s + N_0. \tag{32}$$

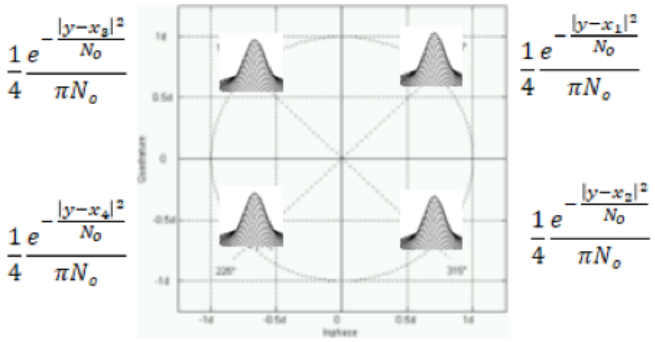

Figure 1. Mixture random variable Y for QPSK data symbol.

Equations (28), (29), and (32) indicate that the output random variable Y is a zero-mean Gaussian mixture of M Gaussian distributions, with variance $E_s + N_0$.

Fig. 1 depicts the distribution of Gaussian mixture Y for QPSK data symbol on a constellation diagram. In this figure, Gaussian noise is sitting on top of each constellation point.

Substituting (4) and (28) into (3), the mutual information is

$$i(x;y) = \log M - \frac{|y-x|^2}{N_0} - \log\left(\sum_{k=1}^{K} e^{-\frac{|y-x_k|^2}{N_0}}\right). \quad (33)$$

Substitute (33) into (5), the average mutual information is given as

$$I(X;Y) = \log M - 1 - I_{YX} \quad (34)$$

where

$$I_{YX} = \frac{1}{MN_0\pi}\sum_{j=1}^{M}\int_{-\infty}^{\infty} e^{-\frac{|y-x_j|^2}{N_0}} \log\left(\sum_{k=1}^{M} e^{-\frac{|y-x_k|^2}{N_0}}\right) dy. \quad (35)$$

Due to the presence of a mixture of Gaussian components, for high order of modulation, QPSK or higher ($M \geq 4$), there is no closed form expression for I_{YX} and the average mutual information [22–24].

The constrained capacity of M-PSK signal that has finite alphabet M, uniformly distributed, it is given by

$$C_{\text{con}} = I(Y;X) \leq C^0. \quad (36)$$

As discussed in Section 2.1, under Gaussian input assumption, the outage probability is governed by the channel capacity. For uniform distribution assumption of the input signal, the outage probability is governed by the constrained capacity. For M-PSK signal, no closed form expression of the constrained capacity. An approximation, a numerical, and a Monte-Carlo simulation solution of the constrained capacity will be used.

Modulation	a	b	L
QPSK	1	0.63	1
8-PSK	0.6130	0.1955	2
	0.3855	0.8992	

Table 1. Approximation parameters of (37) for QPSK and 8-PSK modulations.

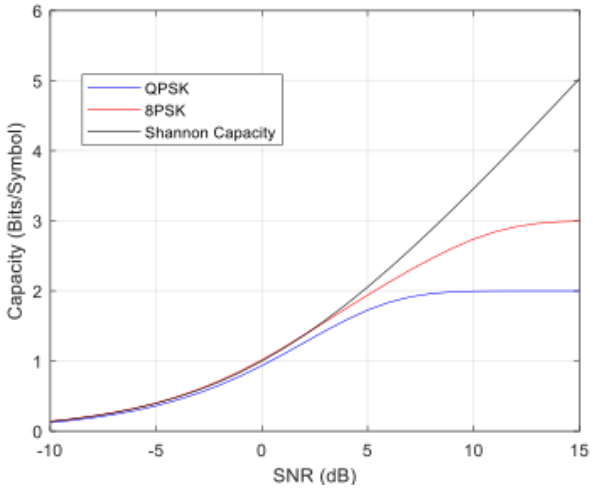

Figure 2. Approximation of Constrained Capacity for QPSK and 8-PSK and Shannon capacity.

2.3. Method 1: Approximation Constrained Capacity for M-PSK Signals

An exponential approximation that reduces the computational burden is given as [25]

$$C_{\text{con}}(\gamma) \approx \log_2 M\left(1 - \sum_{i=1}^{L} a_i e^{-b_i\gamma}\right), \quad (37)$$

where γ denotes the SNR, a_i, b_i, L are curve fitting parameters. Approximation parameters for QPSK and 8-PSK are summa-rized in Table 1.

Fig. 2 depicts the approximate of the constrained capacity for QPSK and 8-PSK modulations and the Shannon capacity.

2.4. Method 2: Numerical Integration Constrained Capacity for M-PSK Signals

To evaluate (35) via numerical integration, make a change of variables

$$s = \frac{y_{\text{R}} - x_{j,\text{R}}}{\sqrt{N_0}}, \text{and } s = \frac{y_{\text{I}} - x_{j,\text{I}}}{\sqrt{N_0}}, \quad (38)$$

where Y_{R} and Y_{I} denote the real and imaginary parts of sample y, respectively; and $x_{j,\text{R}}$ and $x_{j,\text{I}}$ denote the real and imaginary parts of sample x_j, respectively.

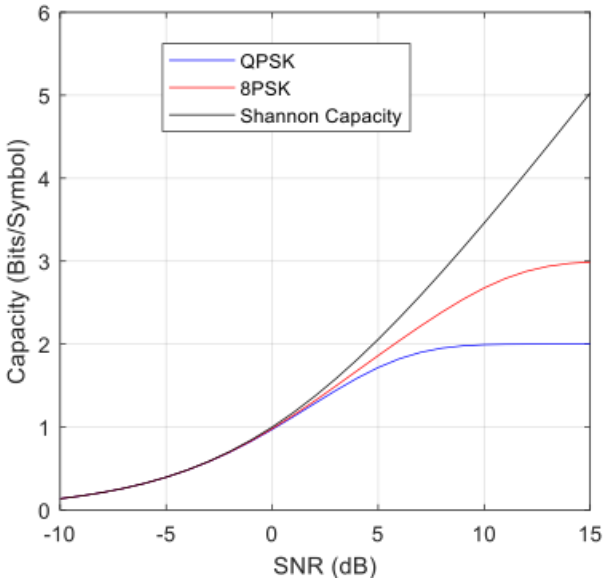

Figure 3. Numerically integration of constrained capacity for QPSK and 8-PSK, and Shannon capacity.

Substituting (38) into (35), one obtains

$$I_{YX} = -\frac{1}{M\pi}\sum_{k=1}^{M}\int_{-\infty}^{\infty}\int_{-\infty}^{\infty} e^{-s^2-t^2} h(s,t)\,ds dt \tag{39}$$

where

$$h(s,t) = \log\left(\sum_{k=1}^{M} e^{-\left[\left(s+\frac{x_{j,R}-x_{k,R}}{\sqrt{N_0}}\right)^2+\left(t+\frac{x_{j,I}-x_{k,I}}{\sqrt{N_0}}\right)^2\right]}\right). \tag{40}$$

Using the Gauss-Hermite quadrature [26] to numerically integrate (39), one obtains

$$I_{YX} \approx -\frac{1}{M\pi}\sum_{j=1}^{N} w_j \sum_{i=1}^{N} v_i h(s_i,t_j), \tag{41}$$

where s_i and t_j are roots of the Hermite polynomial and v_i and w_j are associated weights.

Substituting (41) into (34), one obtains

$$\begin{aligned} C_{\text{con}}(\gamma) &= I(Y;X) \\ &\approx \log M - 1 - \frac{1}{M\pi}\sum_{j=1}^{N} w_j \sum_{i=1}^{N} v_i h(s_i,t_j). \end{aligned} \tag{42}$$

Fig. 3 depicts the numerical integration of constrained capacity for QPSK and 8-PSK modulations and the Shannon capacity.

Follow a similar development to that described in Section 2.1 of the paper, the distribution of the mutual information rate random variable Z_n between the input and output vectors of length n can be expressed as

$$Z_n = \log M - V_n, \tag{43}$$

where

$$V_n = \frac{1}{n}\sum_{k=1}^{n}\frac{|N_k|^2}{N_0} + \frac{1}{n}\sum_{k=1}^{n}\log\left(\sum_{j=1}^{M} e^{-\frac{|Y_k-x_j|^2}{N_0}}\right). \tag{44}$$

Define

$$|Y_k - x_j|^2 \triangleq |Y_k|^2 + \beta|X_j|^2 \tag{45}$$

where

$$|\beta| \le 1. \tag{46}$$

For a single ring constellation of M-PSK signals, we have

$$|x_j|^2 = E_s, \text{ for } j = 1, 2, \ldots, M. \tag{47}$$

Substituting (45) and (47) into (44), after some algebra, one obtains

$$V_n = \log M - \beta\gamma - \frac{1}{n}\sum_{k=1}^{n}\frac{|Y_k|^2}{N_0} + \frac{1}{n}\sum_{k=1}^{n}\frac{|N_k|^2}{N_0}. \tag{48}$$

Substituting (48) into (43), one obtains

$$Z_n = \beta\gamma + \frac{1}{n}\sum_{k=1}^{n}\frac{|Y_k|^2}{N_0} - \frac{1}{n}\sum_{k=1}^{n}\frac{|N_k|^2}{N_0}. \tag{49}$$

Define

$$W_n \triangleq \frac{1}{n}\sum_{k=1}^{n}\frac{|Y_k'|^2}{N_0} - \frac{1}{n}\sum_{k=1}^{n}\frac{|N_k'|^2}{N_0}, \tag{50}$$

where

$$Y_k' = \frac{Y_k}{\sqrt{N_0}} \text{ and } N_k' = \frac{N_k}{\sqrt{N_0}}. \tag{51}$$

Since Y_k is a zero-mean Gaussian mixture, Y_k' is also a zero mean Gaussian mixture, variance equals $\gamma + 1$, while N_k' is a normalized Gaussian random variable, zero mean, variance equals 1. Therefore, W_n is also a zero-mean random variable.

Given (5), (36), (43)–(49), in the mean of (49), one obtains

$$C_{\text{con}}(\gamma) = \beta\gamma. \tag{52}$$

Since $|\beta| \le 1$, we have

$$C_{\text{con}}(\gamma) \le C^0(\gamma) = \log(1+\gamma) \le \gamma. \tag{53}$$

Substituting (50) and (52) into (49), one obtains

$$Z_n = C_{\text{con}} + W_n. \tag{54}$$

Again, C_{con} is obtained by either approximation or numerically methods as given either by (37) and (42), respectively, and W_n is given by (50). The mean of the mutual information rate random variable is governed by the constrained capacity. Again, similar to part I, for $n = 1$ and in the limit where Y follows a Gaussian distribution, W is a Laplacian random variable, with variance depends on γ. When Y is a Gaussian mixture of M Gaussian distributions, the variance of W is M times the variance of a single Gaussian distribution, i.e.,

$$\sigma_W^2 = \frac{2M\gamma}{\gamma + 1}. \tag{55}$$

For large n, $(n > 100)$, using Central Limit Theorem, W_n follows a Gaussian distribution. The mutual information rate random variable Z_n shown in (44) can be expressed as

$$Z_n \sim \mathcal{N}\left(C_{\text{con}}(\gamma), \frac{2M\gamma}{n(\gamma + 1)}\right). \tag{56}$$

Comparing this result against part I, although the distribution of the mutual information rate random variable Z_n is Gaussian; however, the mean shifts toward the constrained capacity and the variance is M times larger.

Proposition 2. For infinite length codeword, the mutual information rate random variable Z_n is the constrained capacity.

Proof. Similar to Part I, taking the limit of the variance of the mutual information rate random variable Z_n as the codeword length approaches infinity, one obtains

$$\lim_{n\to\infty} Var(Z_n) = \lim_{n\to\infty} \frac{2M\gamma}{n(\gamma + 1)} = 0. \tag{57}$$

Thus, the mutual information rate random variable converges to the constrained capacity. □

The outage probability P_{o} is the probability that the mutual information rate is less than the code rate R_e. The outage probability for Z_n is given by

$$P_{\text{o}} = P[Z_n \leq R_e] = F_{Z_n}(R_e), \tag{58}$$

or

$$P_{\text{o}} = Q\left(\frac{C_{\text{con}-R_e}}{\sqrt{2M\gamma/n(\gamma + 1)}}\right). \tag{59}$$

Again, R_e is given by (22). For M-PSK signals, the IOP shown in (59) is applicable for the entire SNR region. Equation (59) provides the performance benchmark for moderate-length codes. Numerical simulation of the DVB-S2 FEC with various code rates and the IOP are discussed in the simulation section of the paper.

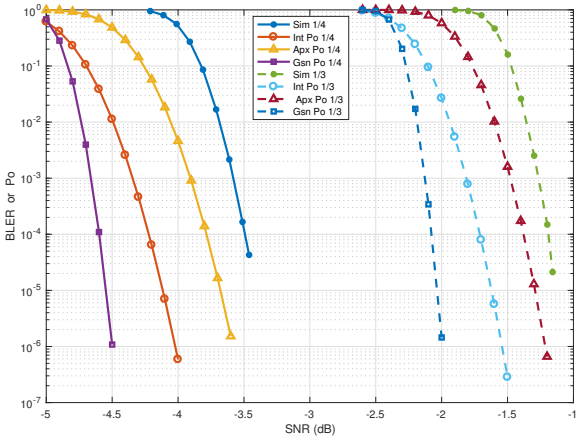

Figure 4. BLER and P_{o} for QPSK, code rate $R_c = \{1/4, 1/3\}$.

As shown above, the mean of the mutual information rate random variable Z_n is a function of constrained capacity. The performance of the outage probability is sensitive to the expected capacity, the degree in which the approximation, numerical integration, and Monte-Carlo simulation methods converge to the expected capacity. We will discuss the performance of the outage probability and numerical results in Section 3 of the paper.

3. Simulation Results

Computer simulations for Quadrature Phase Shift Keying (QPSK) and 8-Phase Shift Keying (8-PSK), using DVB-S2 FEC with a fixed length of 16,200 coded bits, code rates R_c of $1/4$, $1/3$, $1/2$, $2/3$, $3/4$ and $8/9$ are considered. Details information of the DVB-S2 FEC and the constellations of QPSK and 8-PSK are defined in [27].

Fig. 4 depicts the outage probability P_{o} using numerical integration, approximation, Gaussian assumption, and simulated BLER for QPSK with low code rate $R_c = \{1/4, 1/3\}$.

Fig. 5 depicts the outage probability P_{o} using numerical integration, approximation, Gaussian assumption, and simulated BLER for QPSK with moderate code rate $R_c = \{1/2, 2/3\}$.

Fig. 6 depicts the outage probability P_{o} using numerical integration, approximation, Gaussian assumption, and simulated BLER for 8-PSK with high code rate $R_c = \{3/4, 8/9\}$.

As shown in Figs. 4-6, the outage probability curves

- are loose for the Gaussian input distribution assumption. The performance bound increases for either high order of modulation or code rate. Relative to simulated curve, the bound exceeds 3.5 dB for 8-PSK, rate 8/9. It is a direct result of

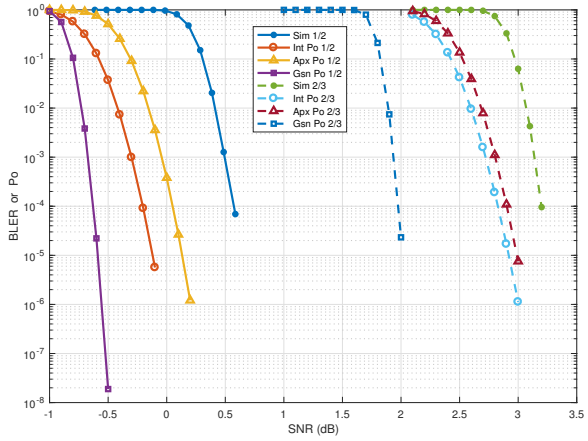

Figure 5. BLER and P_o for QPSK, code rate $R_c = \{1/2, 2/3\}$.

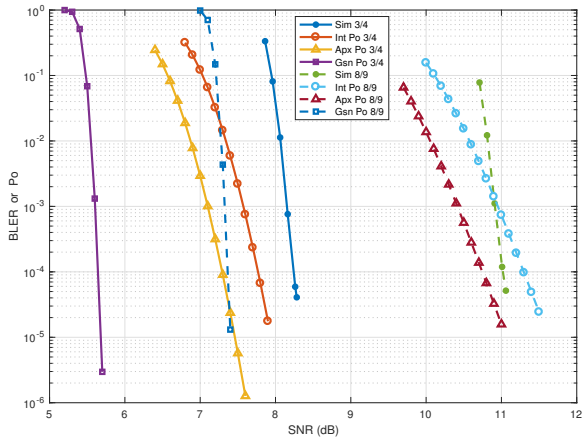

Figure 6. BLER and P_o for QPSK, code rate $R_c = \{3/4, 8/9\}$.

the Shannon capacity that exceeds the constrained capacity, SNR > 5 dB;

- are tight for the numerical constrained capacity method. An interesting observation is for 8-PSK, rate 8/9, the outage probability curve crosses the simulated curve. In this SNR region, the constrained capacity is slightly underestimated; it shifts the outage probability curve to the right and causing its slope more gradual, not as steep as the simulated curve;
- are also tight for the approximate constrained capacity method; with the exception of 8-PSK rate 3/4 where the numerical method is tighter for about 0.5 dB. In this case, the constrained capacity is slightly overestimated.

Table 2 summarizes the performance for all methods at BLER equals 10^{-4}. Results shown in Table II indicate that both the numerical and approximation constrained capacity methods provide the tight bound for the outage probability.

Modulation	R_c	Δ_{Int}(dB)	Δ_{Apx}(dB)	Δ_{Gsn}(dB)
QPSK	1/4	0.73	0.29	1.11
QPSK	1/3	0.52	0.18	0.85
QPSK	1/2	0.78	0.50	1.18
QPSK	2/3	0.35	0.30	1.20
8-PSK	3/4	0.48	0.96	2.57
8-PSK	8/9	−0.27	0.27	3.62

Table 2. Performance bound in dB for the outage probability P_o, using numerical integration, approximation, and Gaussian input distribution assumption at BLER = 10^{-4}.

4. Conclusion

Feinstein's lemma for the IOP is a practical approach and an important benchmark of achievable rate to predict the performance of moderate length codes. In this paper, we presented an approach to compute the IOP for M-PSK signals using DVB-S2 FEC with a fixed length of 16, 200 coded bits with numerous code rates for AWGN channel. Computer simulation, using PTW waveform which employs QPSK and 8-PSK signaling, DVB-S2 FEC with a fixed length of 16, 200 coded bits with numerous code rates were presented to compare the BLER against the outage probability under Gaussian and uniform distributions of the input signals. With the Gaussian inputs distribution assumption, the IOP results in the loosest bound. The bound exists 3.5 dB for 8-PSK, rate 8/9. When the code is operating in the high SNR region Shannon capacity exceeds the constrained capacity. Therefore, for high order of modulation and high code rate, one should not assume Gaussian input distribution. The bound is tight for the numerical constrained method. The performance bound in the range of −0.27 to 0.78 dB for BLER of 10^{-4}. For 8-PSK, rate 8/9, the outage probability curve intersects with the simulated curve. In this region, the numerical constrained capacity is slightly underestimated; it shifts the outage probability curve to the right and causing its slope to be more gradual than the simulated curve. The bound is also tight and consistent for the approximate constrained capacity method. However, the bound peaks for 8-PSK, rate 3/4. In this case, the constrained capacity is slightly overestimated; it causes the outage proba-bility curve shifts to the left, which result in a performance bound of 0.96 dB at BLER of 10^{-4}. For the approximation constrained method, the performance bound is in the range of 0.18 to 0.96 dB for BLER of 10^{-4}. An interesting observation is that one can use the simulated curve to benchmark the rate of convergence for the constrained capacity. Comparing all the methods, for QPSK and 8-PSK with all the

code rates under consideration, both the approximation and numerical methods for constrained capacity yield good predictor for the performance bound of moderate-length codes. The IOP technique presented in the paper can be extended to predict the theoretical benchmark for a wide class of moderate-length codes.

References

[1] L. K. Nguyen, R. B. Wells, D. H. N. Nguyen, and N. H. Tran, "Outage probability and constrained capacity of moderate-length codes for Gaussian mixture over awgn channel," in *IEEE Military Commun. Conf.*, (Los Angeles, CA, USA), Oct. 2018.

[2] S. Verdu and T. S. Han, "A general formula for channel capacity," *IEEE Trans. Inform. Theory*, vol. 40, pp. 1147–1157, July 1994.

[3] C. Shannon, "A mathematical theory of communication," *Bell Labs. Tech. J.*, vol. 27, pp. 379–423, 1948.

[4] A. Feinstein, "A new basic theorem of information theory," *IEEE Trans. Inform. Theory*, vol. 4, no. 4, pp. 2–22, 1954.

[5] L. Ozarow, S. Shamai, and A. D. Wyner, "Information theoretic considerations for cellular mobile radio," *IEEE Trans. Veh. Technol.*, vol. 43, pp. 359–378, May 1994.

[6] A. Guillen i Fabregas and G. Caire, "Coded modulation in the block-fading channel: Coding theorm and code construction," *IEEE Trans. Inform. Theory*, vol. 52, pp. 91–114, Dec. 2006.

[7] K. Niu and Y. Li, "Polar coded diversity on block fading channels via polar spectrum," *IEEE Transactions on Signal Processing*, vol. 69, pp. 4007–4022, 2021.

[8] N. Laneman, "On the distribution of mutual information," in *Proc. Inform. Theory and Its Appl. Workshop*, (San Diego, CA, USA), Feb. 2007.

[9] K. Rajab and F. Kamalov, "Finite sample based mutual information," *IEEE Access*, vol. 9, pp. 118871–118879, 2021.

[10] Y. Bu, S. Zou, and V. V. Veeravalli, "Tightening mutual information-based bounds on generalization error," *IEEE Journal on Selected Areas in Information Theory*, vol. 1, no. 1, pp. 121–130, 2020.

[11] D. Buckingham and M. C. Valenti, "The information-outage probability of finte-length codes over AWGN channel," in *Annual Conf. Inform. Sci. and Syst.*, 2008.

[12] T. S. Han, *Information Spectrum Methods in Information Theory*. Berlin: Springer, 2003.

[13] 4G Americas, *4G Mobile Broadband Evolution: 3GPP Release 11 & Release 12 and Beyond*. PhD thesis, Feb. 2014.

[14] Y. Polyanskiy, H. V. Poor, and S. Verdu, "Channel coding rate in the finite blocklength regime," *IEEE Trans. Inform. Theory*, vol. 56, pp. 2307–2359, May 2010.

[15] M. Mohammadkarimi, R. Schober, and V. W. S. Wong, "Channel coding rate for finite blocklength faster-than-nyquist signaling," *IEEE Communications Letters*, vol. 25, no. 1, pp. 64–68, 2021.

[16] H. Lieske, S. Rauh, and A. Heuberger, "Numerical evaluation of information outage for BPSK FHSS link performance," in *Proc. IEEE Wireless Commun. and Networking Conf.*, pp. 1–6, 2017.

[17] J. Sullivan, M. Glaser, C. Walsh, W. Dallas, J. Blackman, J. VanderVennet, C. Shunshine, and J. C. Chuang, "Protected tactical MILSATCOM design for affordability risk reduction (DFARR) results," in *Proc. IEEE Military Commun. Conf.*, 2014.

[18] B. J. Wolf and J. C. Huang, "Implementation and testing of the protected tactical waveform (PTW)," in *Proc. IEEE Military Commun. Conf.*, 2015.

[19] L. K. Nguyen, M. A. Blanco, and L. J. Sparace Sr., "On the sensitivity of wideband radiometric detection for low probability of intercept and probability of detection (lpi/lpd) in frequency hopped systems," in *Proc. IEEE Military Commun. Conf.*, 2011.

[20] L. K. Nguyen, R. B. Wells, D. H. N. Nguyen, and N. H. Tran, "Outage probability analysis of the protected tactical waveform (PTW) on the return link," in *Proc. IEEE Military Commun. Conf.*, (Baltimore, MD, USA), Oct. 2017.

[21] M. S. Pinsker, *Information and Information Stability of Random Variables and Processes*. Holiday-Day, 1964.

[22] M. Ranjbar, N. H. Tran, H. Nguyen-Le, and T. Karacolak, "Energy efficiency of uplink and downlink non-orthogonal multiple-access channels under gaussian-mixture interference," *IEEE Transactions on Green Communications and Networking*, vol. 4, no. 3, pp. 657–668, 2020.

[23] M. Ranjbar, H. Nguyen-Le, T. Karacolak, and N. H. Tran, "Energy efficiency of noma-based wireless networks under gaussian-mixture interference," in *ICC 2019 - 2019 IEEE International Conference on Communications (ICC)*, pp. 1–6, 2019.

[24] Z. Zhang, Z. Du, and W. Yu, "Mutual-information-based ofdm waveform design for integrated radar-communication system in gaussian mixture clutter," *IEEE Sensors Letters*, vol. 4, no. 1, pp. 1–4, 2020.

[25] P. Yang, Y. Wu, L. Jin, and H. Yang, "Sum capacity for single-cell multi-user systems with m-ary inputs," *Entropy*, vol. 19, no. 9, p. 497, 2017.

[26] M. Abramowitz and I. A. Stegun, *Handbook of mathematical functions: with formulas, graphs, and mathematical tables*. New York: USA: Dover Publications, Inc., 1965.

[27] ETSI EN 302 307 v1.2.1 (2009-08), *Digital Video Broadcasting (DVB); Second generation framing structure, channel coding and modulation systems for Broadcasting, Interactive Services, News Gathering and other broadband satellite applications (DVB-S2)*.